Visual Chirality

Zhiqiu Lin[1] Jin Sun[1,2] Abe Davis[1,2] Noah Snavely[1,2]
Cornell University[1] Cornell Tech[2]

Abstract

How can we tell whether an image has been mirrored? While we understand the geometry of mirror reflections very well, less has been said about how it affects distributions of imagery at scale, despite widespread use for data augmentation in computer vision. In this paper, we investigate how the statistics of visual data are changed by reflection. We refer to these changes as "visual chirality," after the concept of geometric chirality—the notion of objects that are distinct from their mirror image. Our analysis of visual chirality reveals surprising results, including low-level chiral signals pervading imagery stemming from image processing in cameras, to the ability to discover visual chirality in images of people and faces. Our work has implications for data augmentation, self-supervised learning, and image forensics.

1. Introduction

"...there's a room you can see through the glass—that's just the same as our drawing room, only the things go the other way."

— Lewis Carroll,
"Alice's Adventures in Wonderland & Through the Looking-Glass"

There is a rich history of lore involving reflections. From the stories of Perseus and Narcissus in ancient Greek mythology to the adventures of Lewis Carroll's Alice and J.K. Rowling's Harry Potter, fiction is full of mirrors that symbolize windows into worlds similar to, yet somehow different from, our own. This symbolism is rooted in mathematical fact: what we see in reflections is consistent with a world that differs in subtle but meaningful ways from the one around us—right hands become left, text reads backward, and the blades of a fan spin in the opposite direction. What we see is, as Alice puts it, "just the same... only the things go the other way".

Geometrically, these differences can be attributed to a world where distances from the reflecting surface are negated, creating an orientation-reversing isometry with objects as we normally see them. While the properties of such isometries are well-understood in principle, much less is known about how they affect the statistics of visual data at scale. In other words, while we understand a great deal about how reflection changes image data, we know much less about how it changes what we learn from that data—this, despite widespread use of image reflection (e.g., mirror-flips) for data augmentation in computer vision.

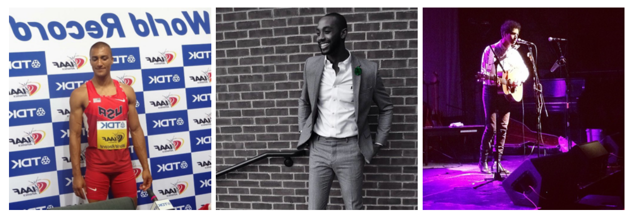

(a) (b) (c)

Figure 1. **Which images have been mirrored?** Our goal is to understand how distributions of natural images differ from their reflections. Each of the images here appears plausible, but some subset have actually been flipped horizontally. Figuring out which can be a challenging task even for humans. Can you tell which are flipped? Answers are in Figure 2.

This paper is guided by a very simple question: How do the visual statistics of our world change when it is reflected? One can understand some aspects of this question by considering the images in Figure 1. For individual objects, this question is closely related to the concept of *chirality* [12]. An object is said to be *chiral* if it cannot be rotated and translated into alignment with its own reflection, and *achiral* otherwise.[1] Put differently, we can think of chiral objects as being fundamentally changed by reflection—these are the things that "go the other way" when viewed through a mirror—and we can think of achiral objects as simply being moved by reflection. Chirality provides some insight into our guiding question, but remains an important step removed from telling us how reflections impact learning. For this, we need a different measure of chirality—one we call *visual chirality*—that describes the impact of reflection on distributions of imagery.

In this paper, we define the notion of visual chirality, and analyze visual chirality in real world imagery, both through new theoretical tools, and through empirical analysis. Our analysis has some unexpected conclusions, including 1) deep neural networks are surprisingly good at determining whether an image is mirrored, indicating a significant degree

[1] More generally, any figure is achiral if its symmetry group contains any orientation-reversing isometries.

(a) (b) (c)

Figure 2. Images from Figure 1 with chirality-revealing regions highlighted. These regions are automatically found by our approach to chiral content discovery. (a, **flipped**) *Text chirality.* Text (in any language) is strongly chiral. (b, **not flipped**) *Object chirality.* The shirt collar, and in particular which side the buttons are on, exhibit more subtle visual chirality. (c, **flipped**) *Object interaction chirality.* While guitars are often (nearly) symmetric, the way we hold them is not (the left hand is usually on the fretboard).

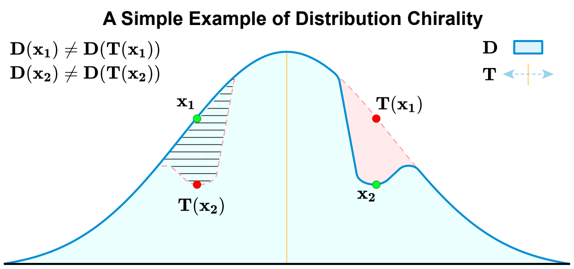

Figure 3. The curve above represents a distribution over images (shown as a 1D distribution for simplicity). Using a transformation $\mathbf{T}$ to augment a sample-based approximation of the distribution $\mathbf{D}$ assumes symmetry with respect to $\mathbf{T}$. We define visual chirality in terms of approximation error induced by this assumed symmetry when $\mathbf{T}$ is image reflection.

of visual chirality in real imagery, 2) we can automatically discover high-level cues for visual chirality in imagery, including text, watches, shirt collars, face attributes, etc, and 3) we theoretically and empirically demonstrate the existence of low-level chiral cues that are imprinted in images by common image processing operations, including Bayer demosaicing and JPEG compression. These conclusions have implications in topics ranging from data augmentation to self-supervised learning and image forensics. For instance, our analysis suggests that low-level cues can reveal whether an image has been flipped, a common operation in image manipulation.

1.1. Defining visual chirality

To define visual chirality, we first consider data augmentation for learning in computer vision to build intuition. Machine learning algorithms are based on the idea that we can approximate distributions by fitting functions to samples drawn from those distributions. Viewed in this light, data augmentation can be seen as a way to improve sampling efficiency for approximating a distribution $\mathbf{D}(\mathbf{x})$ (where $\mathbf{x}$ represents data from some domain, e.g., images) by assuming that $\mathbf{D}$ is invariant to some transformation $\mathbf{T}$. More precisely, augmenting a training sample $\mathbf{x}$ with the function $\mathbf{T}$ assumes symmetry of the form:

$$\mathbf{D}(\mathbf{x}) = \mathbf{D}(\mathbf{T}(\mathbf{x})) \tag{1}$$

which allows us to double our effective sampling efficiency for $\mathbf{D}$ at the cost of approximation error wherever the assumed symmetry does not hold. This idea is illustrated in Figure 3.

Recall that for achiral objects reflection is equivalent to a change in viewpoint. Therefore, if we consider the case where $\mathbf{D}$ is a uniform distribution over all possible views of an object, and $\mathbf{T}$ is image reflection, then Equation 1 reduces to the condition for achirality. We can then define *visual chirality* by generalizing this condition to arbitrary visual distributions. In other words, we define visual chirality as a measure of the approximation error associated with assuming visual distributions are symmetric under reflection. Defining visual chirality in this way highlights a close connection with data augmentation. Throughout the paper we will also see implications to a range of other topics in computer vision, including self-supervised learning and image forensics.

Note that our definition of visual chirality can also be generalized to include other transformations. In this paper we focus on reflection, but note where parts of our analysis could also apply more broadly.

Notes on visual chirality vs. geometric chirality. Here we make a few clarifying observations about visual chirality. First, while geometric chirality is a binary property of objects, visual chirality can be described in terms of how *much* Equation 1 is violated, letting us discuss it as a continuous or relative property of visual distributions, their samples, or, as we will see in Section 4, functions applied to visual distributions. Second, visual chirality and geometric chirality need not imply one another. For example, human hands have chiral geometry, but tend to be visually achiral because the right and left form a reflective pair and each occurs with similar frequency. Conversely, an achiral object with one plane of symmetry will be visually chiral when it is only viewed from one side of that plane. For the remainder of the paper we will refer to geometric chirality as such to avoid confusion.

2. Related work

Chirality has strong connections to symmetry, a long-studied topic in computer vision. Closely related to our work is recent work exploring the asymmetry of *time* (referred to as "Time's arrow") in videos, by understanding what makes videos look like they are being played forwards or backwards [20, 24]—a sort of temporal chirality. We explore the spatial version of this question, by seeking to understand what makes images look normal or mirrored. This spatial chirality is related to other orientation problems in graphics in vision, such as detecting "which way is up" in an image or 3D model that might be oriented incorrectly [23, 4]. Compared to upright orientation, chirality is potentially much more subtle—many images may exhibit quite weak visual chirality cues, including a couple of the images in Figure 1. Upright orientation and other related tasks have also been used as proxy tasks for unsupervised learning of feature representations [5]. Such tasks include the arrow of time task mentioned above [24], solving jigsaw puzzles [19], and reasoning about relative positions of image patches [2].

Our problem represents an interesting variation on the classic task of detecting symmetries in images [15]. As such, our work is related to the detection and classification of asymmetric, chiral objects, as explored by Hel-Or *et al.*in their work on "how to tell left from right" [9], e.g., how to tell a left hand in an image from a right hand. However, this prior work generally analyzed *geometric* chirality, as opposed to the *visual chirality* we explore, as defined above—for instance, a right hand might be geometrically chiral but not visually chiral, while a right hand holding a pencil might visually chiral due to the prevalence of right-handed people.

Our work also relates to work on unsupervised discovery from large image collections, including work on identifying distinctive visual characteristics of cities or other image collections [3, 18] or of yearbook photos over time [6].

Finally, a specific form of chirality (sometimes referred to as *cheirality*) has been explored in geometric vision. Namely, there is an asymmetry between 3D points in front of a camera and points in back of a camera. This asymmetry can be exploited in various geometric fitting tasks [7].

3. Measuring visual chirality

In principle, one way to measure visual chirality would be to densely sample a distribution and analyze symmetry in the resulting approximation. However, this approach is inefficient and in most cases unnecessary; we need not represent an entire distribution just to capture its asymmetry. Instead, we measure visual chirality by training a network to distinguish between images and their reflections. Intuitively, success at this task should be bound by the visual chirality of the distribution we are approximating.

Given a set of images sampled from a distribution, we cast our investigation of visual chirality as a simple classification task. Let us denote a set of training images from some distribution as $C_{\text{positive}} = \{I_1, I_2, \cdots, I_n\}$ (we assume these images are photos of the real world and have not been flipped). We perform a horizontal flip on each image I_i to produce its reflected version I'_i. Let us denote the mirrored set as $C_{\text{negative}} = \{I'_1, I'_2, \cdots, I'_n\}$. We then assign a binary label y_i to each image I_i in $C_{\text{positive}} \cup C_{\text{negative}}$:

$$y_i = \begin{cases} 0 & \text{if } I_i \in C_{\text{negative}}, \text{ i.e., flipped} \\ 1 & \text{if } I_i \in C_{\text{positive}}, \text{ i.e., non-flipped} \end{cases} \quad (2)$$

We train deep Convolutional Neural Nets (CNNs) with standard classification losses for this problem, because they are good at learning complex distribution of natural images [13]. Measuring a trained CNNs performance on a validation set provides insight on the visual chirality of data distribution we are investigating on.

Next we discuss details on training such a network and the techniques we use to discover the sources of visual chriality of the data distribution using a trained model as a proxy.

Network architecture. We adopt a ResNet network [8], a widely used deep architecture for image classification tasks. In particular, we use ResNet-50 and replace the last average pooling layer of the network with a global average pooling layer [16] in order to support variable input sizes.

Optimization. We train the network in a mini-batch setting using a binary cross-entropy loss. We optionally apply random cropping, and discuss the implications of such data augmentation below. We normalize pixel values by per-channel mean-subtraction and dividing by the standard deviation. We use a stochastic gradient descent optimizer [1] with momentum 0.9 and L_2 weight decay of 10^{-5}.

Hyperparameter selection. Finding a suitable learning rate is important for this task. We perform a grid search in the log domain and select the best learning rate for each experiment by cross-validation.

Shared-batch training. During training, we include both I_i and I'_i (i.e., positive and negative chirality versions of the same image) in the same mini-batch. We observe significant improvements in model performance using this approach, in alignment with prior self-supervised learning methods [5].

Discovering sources of visual chirality. If a trained model is able to predict whether an image is flipped or not with high accuracy, it must be using a reliable set of visual features from the input image for this task. We consider those cues as the source of visual chrility in the data distribution.

We use Class Activation Maps (CAM) [26] as a powerful tool to visualize those discriminative regions from a trained model. Locations with higher activation values in CAM make correspondingly larger contributions to predicting flipped images.

Throughout this paper, we visualize these activation maps as heatmaps using the Jet color scheme (red=higher activations, blue=lower activations). We only compute CAM heatmaps corresponding to an image's correct label. Figure 2 shows examples of such class activation maps.

In the following sections, we analyze visual chirality discovered in different settings using the tools described above.

(a) Resizing (b) Random Cropping

Figure 4. **Resizing vs. random cropping as dataset preprocessing**. This figure shows CAM heatmaps for an image from models trained with two preprocessing methods: (a) resizing and (b) random cropping. We observe that the resizing scheme learns cues in the edges or corners of images (note the focus on the lower left corner of (a)), where JPEG encoding can be asymmetric. On the other hand, the random cropping scheme captures the meaningful high-level cue—the chiral shirt collar.

4. The chirality of image processing

When we first attempted to train our model to distinguish between images and their reflections, we quickly observed that the network would find ways to accomplish this task using low-level cues that appeared only loosely correlated with the image's content. Furthermore, the strength of these cues seemed to vary a great deal with changes in how data was prepared. For example, Figure 4 shows two different CAM heatmaps for the same sample image. The left is derived from a network trained on resized data, and the right is derived from a network trained on random crops of the same data. Both maps identify a dark corner of the image as being discriminative, as well as part of the shirt on one of the the image's human subjects. However, these networks appear to disagree about the relative strength of the chiral cues in these regions. This result illustrates how the way we capture and process visual data—even down to the level of Bayer mosaics in cameras or JPEG compression—can have a significant impact on its chirality. In this section and the supplemental material we develop theoretical tools to help reason about that impact, and use this theory to predict what networks will learn in experiments.

4.1. Transformation commutativity

The key challenge of predicting how an imaging process will affect chirality is finding a way to reason about its behavior under minimal assumptions about the distribution to which it will be applied. For this, we consider what it means for an arbitrary imaging transformation $\mathbf{J}$ to preserve the symmetry of a distribution $\mathbf{D}$ (satisfying Equation 1) under a transformation $\mathbf{T}$. There are two ways we can define this. The first is simply to say that if some symmetry exists in the distribution $\mathbf{D}$ then the same symmetry should exist in $\mathbf{D_J}$, the transformation of that distribution by $\mathbf{J}$. The second is to say that if elements $\mathbf{x}_a$ and $\mathbf{x}_b$ are related by $\mathbf{x}_b = \mathbf{T}\mathbf{x}_a$, then this relationship should be preserved by $\mathbf{J}$, meaning $\mathbf{J}\mathbf{x}_b = \mathbf{T}\mathbf{J}\mathbf{x}_a$. In our supplemental material we show that both definitions hold when $\mathbf{J}$ commutes with $\mathbf{T}$, and that the second definition does not hold when $\mathbf{J}$ does not commute with $\mathbf{T}$. With these observations, commutativity becomes a powerful tool for predicting how a given process $\mathbf{J}$ can affect chirality.

4.2. Predicting chirality with commutativity

In our supplemental material we provide a detailed analysis of the commutativity of Bayer demosaicing, JPEG compression, demosaicing + JPEG compression, and all three of these again combined with random cropping. We then show that, in all six cases, our analysis of commutativity predicts the performance of a network trained from scratch to distinguish between random noise images and their reflection. These predictions also explain our observations in Figure 4. While the full details are presented in the supplemental material, some key highlights include:

- Demosaicing and JPEG compression are both individually chiral and chiral when combined.
- When random cropping is added to demosaicing or JPEG compression individually, they become achiral.
- When demosaicing, JPEG compression, and random cropping are all combined, the result is chiral.

This last conclusion is especially surprising—it implies that common image processing operations inside our cameras may leave a *chiral imprint*, i.e., that they imprint chiral cues that are imperceptible to people, but potentially detectable by neural networks, and that these features are robust to random cropping. Thus, these conclusions have implications on image forensics. For instance, our analysis gives us new theoretical and practical tools for determining if image content has been flipped, a common operation in image editing.

Finally, our analysis of how commutativity relates to the preservation of symmetries makes only very general assumptions about $\mathbf{J}$, $\mathbf{T}$, and $\mathbf{D}$, making it applicable to more arbitrary symmetries. For example, Doersch *et al.* [2] found that when they used the relative position of different regions in an image as a signal for self-supervised learning, the networks would "cheat" by utilizing chromatic aberration for prediction. Identifying the relative position of image patches requires asymmetry with respect to image translation. Applied to their case, our analysis is able to predict that chromatic aberration, which does not commute with translation, can provide this asymmetry.

5. High-level visual chirality

While analysis of chiralities that arise in image processing have useful implications in forensics, we are also interested in understanding what kinds of high-level visual content (objects, object regions, etc.) reveals visual chirality, and whether we can discover these cues automatically. As described in Section 4, if we try to train a network from scratch, it invariably starts to pick up on uninterpretable, low-level image signals. Instead, we hypothesize that if we start with a ResNet network that has been pre-trained on ImageNet object classification, then it will have a familiarity with objects that will allow it to avoid picking up on low-level cues. Note, that such ImageNet-trained networks should *not* have features sensitive to specifically to chirality—indeed, as noted above, many ImageNet classifiers are trained using random horizontal flips as a form of data augmentation.

Data. What distribution of images do we use for training? We could try to sample from the space of all natural images. However, because we speculate that many chirality cues have to do with people, and with manmade objects and scenes, we start with images that feature *people*. In particular, we utilize the StreetStyle dataset of Matzen *et al.* [17], which consists of millions of images of people gathered from Instagram. For our work, we select a random subset of 700K images from StreetStyle, and refer to this as the *Instagram* dataset; example images are shown in Figures 1 and 5. We randomly sample 5K images as a test set S_{test}, and split the remaining images into training and validation sets with a ratio of 9:1 (unless otherwise stated, we use this same train/val/test split strategy for all experiments in this paper).

Training. We trained the chirality classification approach described in Section 3 on *Instagram*, starting from an ImageNet-pretrained model. As it turns out, the transformations applied to images before feeding them to a network are crucial to consider. Initially, we downsampled all input images bilinearly to a resolution of 512×512. A network so trained achieves a 92% accuracy on the *Instagram* test set, a surprising result given that determining whether an image has been flipped can be difficult even for humans.

As discussed above, it turns out that our networks were still picking up on traces left by low-level processing, such as boundary artifacts produced by JPEG encoding, as evidenced by CAM heatmaps that often fired near the corners of images. In addition to pre-training on ImageNet, we found that networks can be made more resistant to the most obvious such artifacts by performing random cropping of input images. In particular, we randomly crop a 512×512 window from the input images during training and testing (rather than simply resizing the images). A network trained in such a way still achieves a test accuracy to 80%, still a surprisingly high result.

Training set	Preprocessing	Test Accuracy	
		Instagram	F100M
Instagram	Resizing	0.92	0.57
Instagram	RandCrop	0.80	0.59
Instagram (no-text)	RandCrop	0.74	0.55

Table 1. **Chirality classification performance of models trained on *Instagram*.** Hyper-parameters were selected by cross validation. The first column indicates the training dataset, and the second column the processing that takes place on input images. The last columns report on a held-out test set, and on an unseen dataset (Flickr100M, or F100M for short). Note that the same preprocessing scheme (resize vs. random crop) is applied to both the training and test sets, and the model trained on *Instagram* without text is also tested on *Instagram* without text.

Non-text cues. Examining the most confident classifications, we found that many involved text (e.g., on clothing or in the background), and that CAM heatmaps often predominantly focused on text regions. Indeed, text is such a strong signal for chirality that it seems to drown out other signals. This yields a useful insight: we may be able to leverage chirality to learn a text detector via self-supervision, for any language (so long as the writing is chiral, which is true for many if not all languages).

However, for the purpose of the current analysis, we wish to discover non-text chiral cues as well. To make it easier to identify such cues, we ran an automatic text detector [25] on *Instagram*, split it into text and no-text subsets, and then randomly sampled the no-text subset to form new training and text set. On the no-text subset, chirality classification accuracy drops from 80% to 74%—lower, but still well above chance.

Generalization. Perhaps our classifier learns features specific to Instagram images. To test this, Table 1 (last column) shows the evaluation accuracy of all models (without finetuning) on another dataset of Internet photos, a randomly selected subset of photos from Flickr100M [22]. Note that there is a significant domain gap between *Instagram* and Flickr100M, in that images in our *Instagram* dataset all contain people, whereas Flickr100M features more general content (landscapes, macro shots, etc.) in addition al people. While the performance on Flickr100M is naturally lower than on *Instagram*, our *Instagram*-trained models still perform above chance rates, with an accuracy of 55% (or 59% if text is considered), suggesting that our learned chiral features can generalize to new distributions of photos.

5.1. Revealing object-level chiral features

Inspecting the CAM heatmaps derived from our non-text-trained *Instagram* model reveals a network that focuses on a coherent set of local regions, such as smart phones and shirt pockets, across different photos. To further understand

Figure 5. **Chiral clusters discovered in the Instagram dataset.** Each row shows selected images from a single discovered cluster. Each image is shown with its corresponding CAM heatmap superimposed, where red regions are highly correlated with its true chirality. We discover a range of object-level chiral clusters, such as cellphones, watches, and shirts.

what the network has learned, we develop a way to group the images, as well as their CAM heatmaps, to determine which cues are most common and salient. Inspired by work on mid-level discriminative patch mining [3, 21, 14, 18], we propose a method built upon CAM that we call *chiral feature clustering*, which automatically groups images based on the similarity of features extracted by the network, in regions deemed salient by CAM.

Chiral feature clustering. First, we extract the most discriminative local chiral feature from each image to use as input to our clustering stage. To do so, we consider the feature maps that are output from the last convolutional layer of our network. As is typical of CNNs, these features are maps with low spatial resolution, but with high channel dimensionality (e.g., 2048).

Given an input image, let us denote the output of this last convolutional layer as $\mathbf{f}$, which in our case is a feature map of dimensions $16 \times 16 \times 2048$ $(w \times h \times c)$. Let $\mathbf{f}(x, y)$ denote the 2048-D vector at location (x, y) of $\mathbf{f}$. We apply CAM, using the correct chirality label for the image, to obtain a 16×16 weight activation map A. Recall that the higher the value of $A(x, y)$, the higher the contribution of the local region corresponding to (x, y) to the prediction of the correct chirality label.

We then locate the spatial maxima of A, $(x^*, y^*) = \arg\max_{(x,y)} A(x, y)$ in each image. These correspond to points deemed maximally salient for the chirality task by the network. We extract $\mathbf{f}(x^*, y^*)$ as a local feature vector describing this maximally chiral region. Running this procedure for each image yields a collection for feature vectors, on which we run k-means clustering.

Results of chiral feature clustering. We apply this clustering procedure to our no-text *Instagram* test set, using $k = 500$ clusters. We observe that this method is surprisingly effective and identifies a number of intriguing object-level chiral cues in our datasets. We refer to these clusters as *chiral clusters*. Examples of striking high-level chiral clusters are shown in Figure 5, and include phones (e.g., held in a specific way to take photos in a mirror), watches (typically worn on the left hand), shirt collars (shirts with buttoned collared typically button on a consistent side), shirt pockets, pants, and other objects.

Many of these discovered chiral clusters are highly interpretable. However, some clusters are difficult to understand. For instance, in the face cluster shown in the last row of Figure 5, the authors could not find obvious evidence of visual chirality, leading us to suspect that there may be subtle chirality cues in faces. We explore this possibility in Section 6. We also observe that some clusters focus on sharp edges in the image, leading us to suspect that some low-level image processing cues are being learned in spite of the ImageNet initialization and random cropping.

6. Visual chirality in faces

Inspired by our results on the Instagram dataset in Section 5, we now analyze chirality in face images. To do so, we use the FFHQ dataset [11] as the basis for learning. FFHQ is a recent dataset of 70K high-quality faces introduced in the context of training generative methods. We use 7% of the images as a test set and the remaining images for training and validation. We train various models on FFHQ, first downsampling images to a resolution of 520×520, then randomly cropping to 512×512. We train a standard model starting from ImageNet pre-trained features. This model achieves an accuracy of 81%, which is a promising indicator that our network can indeed learn to predict the chirality of faces with accuracy significantly better than chance.

However, perhaps there is some bias in FFHQ that leads to spurious chirality signals. For instance, since a face detector is used to create FFHQ, there is the possibility that the detector is biased, e.g., for left-facing faces vs. right-facing faces. To test this, we evaluate how well our FFHQ-trained model generalizes to other independent datasets. In particular, we evaluate this model (without fine-tuning) on another dataset, LFW, a standard face dataset [10]. We upsample the low-resolution images in LFW to 512×512 to match our input resolution. This yields an accuracy of 60%—not as high as FFHQ, perhaps due to different distributions of faces, but still significantly better than chance.

To qualitatively explore the chirality cues the model has identified, we show a sample of chiral clusters derived from the FFHQ test set in Figure 6. We can see that the CAM heatmaps in each cluster focus on specific facial regions. Based on these cluster, we have identified some intriguing preliminary hypotheses about facial chirality:

Hair part. The first cluster in Figure 6 indicates a region around the part of the hair on the left side of the forehead. We conjecture that this could be due to bias in hair part direction. We manually inspected a subset of the FFHQ test set, and found that a majority of people pictured parted their hair from left to right (the ratio is ∼2:1 for photos with visible hair part), indicating a bias for asymmetry in hair, possibly due to people preferentially using their dominant right hand to part their hair.

Predominant gaze direction, aka ocular dominance[2]. The second cluster cluster in Figure 6 highlights a region around the corner of the right eye. We conjectured that this may have to do with bias in gaze direction, possibly due to ocular dominance. We use gaze detection software[3] to determine and compare the locations of the pupil in the left and right eyes. We found that indeed more than two thirds of people in portrait photographs gaze more towards the left.

[2] https://en.wikipedia.org/wiki/Ocular_dominance
[3] https://github.com/shaoanlu/GazeML-keras

Figure 6. **Chiral clusters found in FFHQ.** It shows 3 chiral clusters of FFHQ dataset. The leftmost image of each row is the average face + CAM heatmap for all non-flipped images inside the each cluster. We also show some random non-flipped examples for each cluster.

Note that there are also other clusters left to be explained (for example the "beard" cluster, which may perhaps be due to males tending to use right hands to shave or groom their beard). Exploring such cues would make for interesting future work and perhaps reveal interesting asymmetries in our world.

7. Conclusion

We propose to discover visual chirality in image distributions using a self-supervised learning approach by predicting whether a photo is flipped or not, and by analyzing properties of transformations that yield chirality. We report various visual chirality cues identified using our tool on a variety of datasets such as Instagram photos and FFHQ face images. We also find that low-level chiral cues are likely pervasive in images, due to chiralities inherent in standard image processing pipelines. Our analysis has implications in data augmentation, self-supervised learning, and image forensics. Our results implies that visual chirality indeed exists in many vision datasets and such properties should be taken into account when developing real-world vision systems. However, our work suggests that it can also be used as a signal that can be leveraged in interesting new ways. For instance, since text is highly chiral, our work points to interesting future direction in utilizing chirality in a self-supervised way to learn to detect text in images in the wild. We hope that our work will also inspire further investigation into subtle biases imprinted our visual world.

Acknowledgements. This research was supported in part by the generosity of Eric and Wendy Schmidt by recommendation of the Schmidt Futures program.

References

[1] L. Bottou. Stochastic gradient descent tricks. In *Neural networks: Tricks of the trade. Springer*, page 421–436, 2012. 3

[2] C. Doersch, A. Gupta, and A. A. Efros. Unsupervised visual representation learning by context prediction. *ICCV*, 2015. 3, 4

[3] C. Doersch, S. Singh, A. Gupta, J. Sivic, and A. A. Efros. What makes Paris look like Paris? *SIGGRAPH*, 31(4), 2012. 3, 7

[4] H. Fu, D. Cohen-Or, G. Dror, and A. Sheffer. Upright orientation of man-made objects. In *SIGGRAPH*, 2008. 3

[5] S. Gidaris, P. Singh, and N. Komodakis. Unsupervised representation learning by predicting image rotations. In *ICLR*, 2018. 3

[6] S. Ginosar, K. Rakelly, S. Sachs, B. Yin, and A. A. Efros. A Century of Portraits: A visual historical record of american

high school yearbooks. In *ICCV Workshops*, December 2015. 3

[7] R. Hartley. Cheirality invariants. In *Proc. DARPA Image Understanding Workshop*, 1993. 3

[8] K. He, X. Zhang, S. Ren, and J. Sun. Deep residual learning for image recognition. In *CVPR*, pages 770–778, 2016. 3

[9] Y. Hel-Or, S. Peleg, and H. Hel-Or. How to tell right from left. In *CVPR*, 1988. 3

[10] G. B. Huang, M. Ramesh, T. Berg, and E. Learned-Miller. Labeled faces in the wild: A database for studying face recognition in unconstrained environments. Technical Report 07-49, University of Massachusetts, Amherst, October 2007. 7

[11] T. Karras, S. Laine, and T. Aila. A style-based generator architecture for generative adversarial networks. *CoRR*, abs/1812.04948, 2018. 7

[12] W. T. Kelvin. The molecular tactics of a crystal. *J. Oxford Univ. Jr. Sci. Club*, 18:3–57, 1894. 1

[13] A. Krizhevsky, I. Sutskever, and G. E. Hinton. ImageNet classification with deep convolutional neural networks. In *NeurIPS*, 2012. 3

[14] Y. Li, L. Liu, C. Shen, and A. van den Hengel. Mid-level deep pattern mining. In *CVPR*, 2015. 7

[15] Y. Liu, H. Hel-Or, C. S. Kaplan, and L. J. V. Gool. Computational symmetry in computer vision and computer graphics. *Foundations and Trends in Computer Graphics and Vision*, 5(1-2):1–195, 2010. 3

[16] Q. C. M. Lin and S. Yan. Network in network. In *International Conference on Learning Representations*, pages 2921–2929, 2014. 3

[17] K. Matzen, K. Bala, and N. Snavely. StreetStyle: Exploring world-wide clothing styles from millions of photos. *CoRR*, abs/1706.01869, 2017. 5

[18] K. Matzen and N. Snavely. BubbLeNet: Foveated imaging for visual discovery. In *ICCV*, 2015. 3, 7

[19] M. Noroozi and P. Favaro. Unsupervised learning of visual representations by solving jigsaw puzzles. In *ECCV*, 2016. 3

[20] L. C. Pickup, Z. Pan, D. Wei, Y.-C. Shih, C. Zhang, A. Zisserman, B. Schölkopf, and W. T. Freeman. Seeing the arrow of time. In *CVPR*, 2014. 2

[21] S. Singh, A. Gupta, and A. A. Efros. Unsupervised discovery of mid-level discriminative patches. In *ECCV*, 2012. 7

[22] B. Thomee, D. A. Shamma, G. Friedland, B. Elizalde, K. Ni, D. Poland, D. Borth, and L.-J. Li. Yfcc100m: The new data in multimedia research. *CACM*, 59(2), Jan. 2016. 5

[23] A. Vailaya, H. Zhang, C. Yang, F.-I. Liu, and A. K. Jain. Automatic image orientation detection. *Trans. Image Processing*, 11(7):746–55, 2002. 3

[24] D. Wei, J. Y. S. Lim, A. Zisserman, and W. T. Freeman. Learning and using the arrow of time. In *CVPR*, 2018. 2, 3

[25] H. W. Y. W. S. Z. W. H. X. Zhou, C. Yao and J. Liang. East: An efficient and accurate scene text detector. In *CVPR*, 2017. 5

[26] B. Zhou, A. Khosla, A. Lapedriza, A. Oliva, and A. Torralba. Learning deep features for discriminative localization. In *Proceedings of the IEEE conference on computer vision and pattern recognition*, pages 2921–2929, 2016. 3